

MULTIPARTICLE DYNAMICS 2004

WOLFGANG OCHS

Max-Planck-Institut für Physik, Werner-Heisenberg-Institut
Föhringer Ring 6, D-80805 München, Germany

We summarize results presented at this conference with special emphasis on hard processes with jets and heavy quarks, soft particle production, small x structure functions and diffraction as well as heavy ion collisions and quark gluon plasma.

1. Introduction

In high energy collisions of leptons, hadrons and nuclei we observe the production of many particles, mainly hadrons. The ultimate goal in multiparticle production studies is the explanation of the hadronic phenomena within QCD, the basic theory of the strong interactions, along with the other interactions of the standard model and possibly beyond.

A basic problem in the QCD study of multiparticle production is the matching of parton and hadron dynamics relevant in the respective weak and strong coupling regimes of QCD. A class of inclusive observables in hard collisions can be computed perturbatively in terms of the running coupling constant α_s thanks to the celebrated asymptotic freedom [1]. In practice, it is often required to include some additional non-perturbative input from other sources (*e.g.* Parton Distribution Functions). Hadronic phenomena can be systematically analysed within lattice gauge theory in sufficiently simple problems. The description of genuine multi-hadron production requires, in addition to the hard QCD part (shower calculus), some phenomenological approaches: specific hadronization models or such simple ideas as “parton hadron duality”. At present, the systematic approach to multi-hadron production based entirely on QCD remains a dream. Is it just a problem of complexity or do we need a fundamentally new insight?

In this talk we concentrate on the four topics mentioned in the abstract which represent different variants of the interplay of hard and soft interactions and we emphasise shortly other topics. I am sorry for the incomplete coverage of the many interesting presentations at this conference.

2. Hard processes with jets and heavy quarks

Results are reported from TEVATRON, HERA, RHIC and LEP accelerators. Of central importance is the comparison with fixed order perturbation theory to test the universality of the coupling constant $\alpha_s(Q^2)$ in all processes. Here the goal is to improve the accuracy of the calculation, in particular by the extension beyond Next-to-Leading-Order accuracy, and to compute within the QCD framework observables of higher complexity. An important goal is also the discovery of new physics either through the deviation of experimental results from the precision calculations or through better understanding of background processes.

Top quark production (D. Bauer) has been studied at the TEVATRON $p\bar{p}$ collider where in the new RUN II the cms energy is increased from 1.8 to 1.96 TeV. Top quarks at these energies are produced primarily in pairs and they decay through $t \rightarrow Wb$. The various decay channels for the W have been analysed by both experiments and consistent results have been obtained in eight channels, all compatible with the theoretical computations beyond NLO of $\sigma_{top} = 6.77 \pm 0.42$ pb at $m_t = 175$ GeV [2]. A new value for the top quark mass has been presented by D0 [3] from a reanalysis of their earlier RUN I data: $m_t = 180.1 \pm 3.6(\text{stat.}) \pm 3.9(\text{syst.})$ GeV with considerably reduced errors and this result increases the world average by 4 GeV to $m_t = 178 \pm 4.3$ GeV. The best RUN II CDF result so far obtained is $m_t = 177.8_{-5.0}^{+4.5} \pm 6.2$ GeV. No single top production has been observed and $\sigma_t < 8.5$ pb at 95% CL (RUN II, CDF).

Single top production (S.D. Ellis). The observation of this process would determine the CKM matrix element V_{tb} and be important in other searches (Higgs, new particles, including extra scalar bosons or gauge bosons, new quarks). The expected rates are still below the presently achieved sensitivity. Therefore some strategies to obtain an improved signal/background ratio are proposed, especially by using the “signed rapidity” variable which takes into account the fact that processes with W ’s are not separately C or P invariant.

Jet Production at the TEVATRON (L. Sawyer) is measured now at the higher cms energy by CDF and D0. Single inclusive jets are studied up to transverse momenta $p_T \sim 550$ GeV, that is 150 GeV higher than in RUN I and di-jet masses up to $M_{ij} \sim 1400$ GeV, also the azimuthal decorrelation of the two jet events which is an effect of $\mathcal{O}(\alpha_s)^3$ is measured. These results are found in an overall consistency with the NLO QCD predictions [4, 5] in the extended regime of energy and transverse momentum within the systematic errors which are dominated by the energy scale uncertainty. Only in extreme kinematic regions of the azimuthal decorrelation deviations appear.

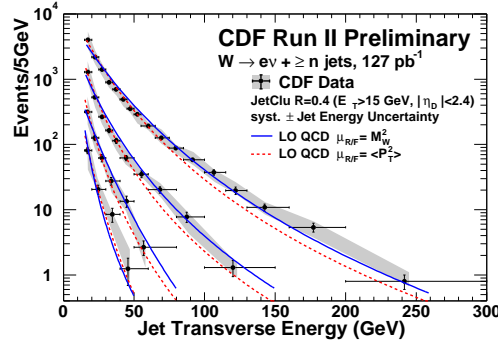


Fig. 1. Distribution of the jet E_T for the jet of lowest energy in the $W + \geq n$ jet sample, for $n=1$ (top) to $n=4$ (down), in comparison with LO QCD calculations.

Production of $W, Z, \gamma + jets$ (A. Cruz) allows further tests of pQCD at large momentum transfers using different techniques. The inclusive W production cross section rises from 2.38 ± 0.24 nb at 1.8 TeV to 2.64 ± 0.18 nb at 1.96 TeV and is well described by the NNLO QCD results of 2.5 and 2.73 nb respectively. For the production of W together with n jets the distribution of the jet transverse energies have been measured. There is good agreement with a calculation (ALPGEN [6]) based on leading order QCD Matrix Element combined with parton shower development (HERWIG [7]), see Fig. 1. Here the experimental uncertainties from the jet energy scale are comparable in size to the theoretical scale uncertainties. *Central di-photon production* has been measured up to masses of about 30 GeV. The NLO QCD calculations (DIPHOX [8]) involving the $q\bar{q}$ annihilation and quark loop diagram for $gg \rightarrow \gamma\gamma$ describe the data well in absolute normalization. The *associated production of photon with heavy flavours* (c, b) has been obtained as well for photon energies up to 60 GeV. It agrees with a LO calculation (Pythia [9]).

In summary for TEVATRON, no serious disagreement of the new data with QCD expectations at different levels of accuracy for the observables of different levels of complexity are met and so, at the same time, we do not obtain any signal of a new physics. The other problems discussed here concern the role of the “underlying event” (*R.D. Field*, see below) and the influence of the selection of jets by a particular algorithm (“cone” vs. “ K_T ”) (*Andrieu*).

Monte Carlo generators, (*L. Lönnblad*) are being developed to generate parton final states beyond LO for present accelerators but also for the LHC. For problems like production of multi-jet or W +jet events a matching of

the NLO matrix element and parton shower has been achieved; also double scattering effects are being considered.

Fragmentation functions (*S. Kretzer*) $D_{q,g}^{h\pm}(z, Q^2)$ are compared in pp and e^+e^- collisions as a tests the collinear factorization approach of QCD at NLO together with universality. New data obtained at RHIC on $pp \rightarrow \pi X$ are well predicted using the previous results [10, 11] from e^+e^- collisions on $D_{q,g}^{h\pm}$ at the factorization scale and subsequent DGLAP evolution.

Jet production at HERA (*C. Glasman*) has now been measured down to $x \simeq 10^{-4}$ for momentum transfers Q^2 larger than a few GeV^2 . The Q^2 dependence of of two- and three-jet cross sections in NC DIS up to $Q^2 \sim 5000 \text{ GeV}^2$, obtained by ZEUS, is found in good agreement with NLO ($\mathcal{O}(\alpha_s^2)$ and $\mathcal{O}(\alpha_s^3)$) predictions. The ratio of both results provides an accurate test of the theory and in particular a precise determination of the coupling constant $\alpha_s(M_Z) = 0.1179 \pm 0.0013$ (stat.) $^{+0.0028}_{-0.0046}$ (exp.) which by itself compares well with the current world average $\alpha_s(M_Z) = 0.1182 \pm 0.0027$ [12] but there is still a large theoretical error of $(+0.0061, -0.0047)$.

Of special interest, also in view of further applications to small x physics, is a test of the validity of the DGLAP approximation to the Q^2 evolution of structure functions. If jets are produced “forward” (in direction of incoming proton) and have transverse energies $(E_T^{jet})^2$ of order Q^2 then the kinematic configuration is not in favour of intermediate gluon emission with strong k_T ordering as is typical for DGLAP evolution and deviations from DGLAP based predictions are expected [13]. Indeed, if jets are selected by the H1 collaboration with $0.5 < (E_T^{jet})^2/Q^2 < 5$ and $x < 0.004$, then the “direct” NLO QCD predictions (DISENT [14]), *i.e.* without photon structure, are too low by about a factor 3 for very small $x < 0.001$. Considerable improvement, although not full agreement, is obtained if a photon structure is included in the DGLAP calculation. If one of the two scales E_T or Q^2 is large compared to the other one the DGLAP factorization approach works best. Whereas work continues to develop the approximations beyond DGLAP, there is no serious conflict with pQCD at the fundamental level.

Spin physics. The spin program at RHIC (*E. Sichtermann*) aims at a measurement of of hard and soft processes with polarised protons. The single transverse spin asymmetry A_N of forward π^0 production has been observed at FNAL at $\sqrt{s} = 20$ and the first results from RHIC show that it persists at $\sqrt{s} = 200 \text{ GeV}$. New results are also presented from the HERMES experiment at DESY (*I. Gregor*) on the study of the transverse single-spin asymmetries in semi-inclusive pion production in DIS. This allows the determination of the protons “transversity” distribution, which represents the degree to which the quarks are polarised along the proton spin transversely polarized to the virtual photon.

3. Soft particle production in hard collisions

The classical applications of pQCD concern observables for hard processes where the hadrons are either summed over or collected into jets so that fixed order perturbation theory can be applied, as in the previous section. A further development, surprisingly successful, is the application of pQCD to observables calculated from the individual momenta of hadrons in the final state directly and in general involves a resummation of the perturbation theory. One has to include some assumptions on the transition from partons to hadrons and eventually on some non-perturbative aspects of colour confinement. There are final state parton observables, like event shapes, which are infrared and collinear safe, i.e. their values do not change if a collinear or soft gluon is added. They are less sensitive to soft hadronization effects. More sensitive are multiplicity observables, such as particle flows inside jets or between jets which are not infrared safe. These observables are a testing ground for “parton hadron duality” ideas (review by *Yu. Dokshitzer*).

3.1. Infrared and collinear safe observables

Event shapes (Yu. Dokshitzer): These observables describe global properties of hadronic final states, in e^+e^- annihilation, for example, one defines “thrust”, “jet mass”, “broadening” and others. The analysis of these observables in perturbation theory (an asymptotic expansion) leads to a description which combines perturbative and non-perturbative aspects, the latter ones represented by a power correction $\propto (1/Q)$ [15]. This term involves an integral over gluon emissions at small transverse momenta k_T where the coupling constant $\alpha_s(k_T^2)$ is ill defined. It is assumed that this integral is finite and - as the coupling itself - universal for the different observables. One therefore introduces the parameter $\alpha_0 = \frac{1}{\mu_I} \int_0^{\mu_I} dk_T \alpha_s(k_T^2)$ at the matching scale μ_I to describe the influence from the soft region [16]. This result, strictly obtained for partons, is then applied to the experimental hadronic observables assuming a duality between both descriptions. The calculation has been extended to the differential distribution of shape observables where the non-perturbative effects can shift or squeeze the perturbative spectra by an amount given by $1/Q$. By now, the fits to event shapes in e^+e^- with two parameters provide a competitive determination of α_s with an error of $\sim 8\%$ and the universality of the non-perturbative parameter $\alpha_0 \sim 0.5$ at $\mu_I = 2 \text{ GeV}$ is confirmed within $\sim 15\%$.

Angularities (G.Sterman): A new class of event shapes allows specific tests for the non-perturbative corrections. From the angles θ_i of the particles

to the thrust axis and energies E_i one constructs the quantity [17]

$$\tau_a = \frac{1}{Q} \sum_i E_i (\sin \theta_i)^a (1 - |\cos \theta_i|)^{1-a} \quad (1)$$

which interpolates between thrust ($a = 0$) and broadening ($a = 1$). Again, one can separate a contribution from soft gluon emission which is then represented by a non-perturbative “shape function” $f_{a,NP}$. It represents corrections of all higher orders in Λ/Q which should be more appropriate near the collinear limit. This represents a generalization of the correction α_0/Q above, which corresponds to a shift of the distribution. Once determined at a particular energy one obtains predictions for other energies.

Interjet radiation: non-global log’s. In DIS and hadron-hadron collisions one is led to consider gluon radiation in part of the phase space excluding a region around the beam direction, so energy flow or event shapes are non-global. Such observables obtain contributions from multi-soft emissions which lead to “non-global log’s”, single logarithmically enhanced contributions [18]. The difficulty is that the number of jets is not fixed. This problem can be tamed by construction of a correlation of the energy flow with an event shape which fixes the number of jets [17, 19].

Automated resummation (G. Zanderighi): In order to facilitate the calculation of new shape observables, in particular for $p\bar{p}$ and DIS, a program (CAESAR [20]) has been developed which, for a class of observables, yields resummed results in NLL order by combining analytical and numerical methods. The limitations concern certain properties in the infrared and collinear limit of the emission (“recursively IRC-safe”) and the dependence on transverse momentum (“continuously global”). Old results have been reproduced, new observables derived, for example, the distribution of global transverse thrust $T_\perp = \frac{1}{E_T} \max_{\vec{n}_T} \sum_i |\vec{p}_{t_i} \vec{n}_T|$ constructed from the transverse momenta with respect to the beam axis. Such calculations open up the possibility to considerably extend the kinematic range of these QCD studies towards the higher energies of TEVATRON and LHC.

3.2. Multiplicities, particle flows

These observables are not infrared safe: emission of a soft gluon would increase the multiplicity by +1. Finite perturbative results for the parton cascade can be obtained by introducing a cut-off $k_T \geq Q_0$. For $Q_0 \gg \Lambda$ the partons represent jets and Q_0 can be viewed as jet resolution in the sense of the “ k_T -algorithm”, one can also take the small $Q_0 \gtrsim \Lambda$ and compare the resulting cascade directly with the hadronic final state in the sense of a duality picture (“Local Parton Hadron Duality” [21]), then Q_0 is a non-perturbative parameter.

Multiplicities in quark and gluon jets at LEP (K. Hamacher) and TEVATRON (A. Pronko): At LEP the multiplicity of gluon jets is determined from 3 jet events after subtraction of 2 jet events at a reduced scale (DELPHI) or from 3 jet events using a boost algorithm (OPAL [22]). The quark jet multiplicity is found directly from the total e^+e^- multiplicity. Theoretical results are obtained from resummed perturbation theory. One approach is based on coupled evolution equations of quark and gluon jets in Modified Leading Logarithmic Approximation [21] which includes fully the $\sqrt{\alpha_s}$ -correction up to NLL order. These calculations reproduce the multiplicity rise with energy. The ratio $r = N_g/N_q$ obtains large corrections beyond MLLA and is reduced from the asymptotic value $r = C_A/C_F = 9/4$ to $r = 1.7$ in 3NLLO [23] and to $r = 1.5$, observed at LEP, in the numeric solution [24] where the only parameters Λ, Q_0 are fit by the total e^+e^- multiplicity. Another calculation is based on the colour dipole model which treats the evolution of dipoles in NLL approximation and includes recoil effects [25]. It describes the data well using an additional non-perturbative parameter.

The CDF Collaboration has separated quark and gluon jets by analysing di-jet and $\gamma + \text{jet}$ events with known jet compositions. The multiplicity data are found generally well consistent with e^+e^- results. The multiplicities reach the higher energies $Q \sim 300$ GeV where they also follow the 3NLLA expectations.

Particles with low momenta in jets (A. Pronko), measured by CDF, show the so-called hump-backed plateau in the variable $\xi = \log(1/x)$ [21] with the suppression of the low energy, large ξ particles because of soft gluon coherence. Results on the ratio $r(\xi)$ of these spectra for gluon over quark jets for $\xi > 3$ approach ratios of $r(\xi) \sim 1.8 \pm 0.2$ again in good agreement with OPAL results. Although larger than for the full jet result ($r \sim 1.5$) it is still below $r(\xi) = C_A/C_F$ expected in [26] for this limit from the dominance of the primary gluon emission. This discrepancy is likely due to the difficulty to obtain "pure" gluon jets, rather, soft particles are emitted from all participating jets of the event. This problem is avoided in

Soft particle emission in 3-jet events in e^+e^- (Hamacher). The particle multiplicity N_3 in a cone perpendicular to the production plane is studied as function of the inter-jet angles Θ_{ij} . The gluon radiation into this cone coherently emitted from the $q\bar{q}g$ "antenna", normalized by a corresponding multiplicity N_2 in 2-jet events, is given by the simple expression [26]

$$\frac{N_3}{N_2} = \frac{C_A}{C_F} r_t = \frac{1}{4} \frac{C_A}{C_F} \left[(1 - \cos \Theta_{qg}) + (1 - \cos \Theta_{\bar{q}g}) - \frac{1}{N_C^2} (1 - \cos \Theta_{q\bar{q}}) \right] \quad (2)$$

The first two leading terms represent the dipoles along the qg directions, in close analogy to QED electric dipoles, except for the colour factors. The

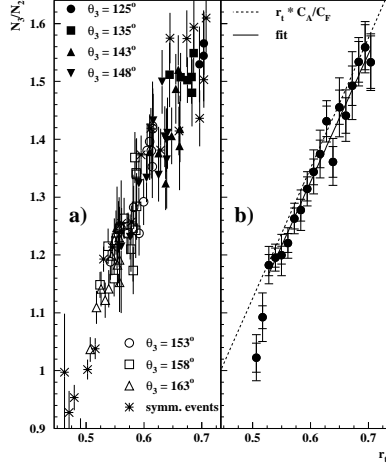


Fig. 2. Multiplicity ratio N_3/N_2 in cones of 30° opening angle as function of r_t in Eq.(2): a) for different inter-jet angles θ_3 ; b) averaged over θ_3 , the dashed line is the expectation Eq.(2) with slope C_A/C_F , the full line is a fit (DELPHI [27]).

formula interpolates for aligned partons between a colour triplet antenna (q against qg) and a colour octet antenna ($q\bar{q}$ against g) with the intensity higher by C_A/C_F .

DELPHI has measured the ratio N_3/N_2 against the variable r_t (see Fig. 2) which shows the scaling behaviour in the angles implicit in (2) and the linear dependence with slope 2.211 ± 0.014 (*stat.*) ± 0.053 (*syst.*) well consistent with the expected slope C_A/C_F [27]. The data are sensitive to the small term $\propto 1/N_C^2$ which corresponds to a negative interference not accessible through purely probabilistic jet algorithms. It is remarkable that the perturbative calculations describe production of particles with such low momenta (few 100 MeV above threshold) at low multiplicity.

Similar transverse effects are expected for γp collisions ($q\bar{q}$ antenna in direct, gg in resolved processes) and $p\bar{p}$ collisions (low transverse radiation in direct γ or W production, high radiation in gluon jet production).

Underlying event in $p\bar{p}$ collisions (R.D. Field): Soft particle production in central rapidity perpendicular to the high p_T trigger jet direction increases rapidly with the jet transverse momentum from low p_T (like minimum bias) up to about 7 GeV and saturates beyond. The same is observed for the transverse momentum sum in back-to-back jet events. If one triggers in addition on a particle in transverse direction one observes the “birth” of a third jet in the same and possibly even on a fourth jet in the opposite direction. This conclusion is derived from the good agreement with the

PYTHIA MC which includes multiple parton collisions whereas HERWIG without this addition is in a less good agreement. It will be interesting in future studies to clarify the role of multi-parton scattering and also to investigate the possible reduction of the transverse particle production in direct γ and W production processes as expected for the perturbative gluon radiation mechanism emphasized in the previous paragraph for e^+e^- collisions.

4. Small x structure functions and diffraction

There is an old expectation for the parton density at small x to “saturate” [28], i.e. to become so high that a limiting behaviour related to the finite proton (or nuclear) size is reached. Ultimately, one expects a transition into a strong coupling regime not accessible to perturbative treatment. With the new data from HERA and RHIC this debate enters a new round. The “Pomeron” which describes diffractive processes with vacuum quantum number exchange is treated as composite object with a partonic sub-structure.

4.1. Deep Inelastic Scattering and parton saturation

In the standard perturbative treatment of DIS (DGLAP 1972-1977) the photon interacts with the proton through exchange of a single parton ladder which leads to a linear evolution equation of the parton densities in Q^2 . With decreasing Bjorken x there is the possibility of multiple interaction of photon and proton through exchange of two or more parton ladders as described by GLR [28] (1983). This happens for sufficiently large parton overlap probability $W(x, Q^2)$, given by the ratio of the parton parton cross section at scale Q^2 , $\hat{\sigma} \sim \frac{\alpha_s(Q^2)}{Q^2}$, to the mean distance of two partons in the proton, $\Delta\vec{b}^2 \sim \frac{F(x, Q^2)}{\pi R^2}$ for proton radius R and parton density $F(x, Q^2) \sim xG(x, Q^2)$. While for $W \ll 1$ the DGLAP approximation is appropriate, for $W \sim \alpha_s$ the non-linear recombination processes set in and, ultimately, at $W = 1$ saturation is reached, i.e. a full overlap of partons in the proton which is beyond perturbation theory. This limit defines the characteristic saturation scale $Q_s(x)$ from

$$\frac{xG(x, Q_s^2)}{\pi R^2} \sim \frac{Q_s(x)^2}{\alpha_s(Q_s^2)} \quad (3)$$

For small α_s this corresponds to a state of high gluon density.

The theoretical analysis starts from the dipole picture [29], formulated in space time, from which the γ^*p total cross section can be computed as

$$\sigma_{T,L}^{\gamma^*p}(x, Q^2) = \int d^2r \int dz \hat{\sigma}_{\text{dipole}}(\vec{r}, x) |\psi_{T,L}^{\gamma}(\vec{r}, z, Q^2)|^2 \quad (4)$$

where ψ^{γ} is the wave function of the virtual photon splitting into a $q\bar{q}$ dipole, z the photon longitudinal momentum fraction of the quark and r the transverse size of the dipole.

Different approaches are used for the dipole cross section. The scattering process can be studied in the proton rest frame and one considers higher orders to the $q\bar{q}$ wave function. A non-linear evolution equation for the dipole-proton scattering amplitude has been given by Balitsky and by Kovchegov [30]. A complementary approach treats the gluons at small x in an effective field theory in a frame with a low momentum photon and an energetic proton where the partonic motions in the proton are largely frozen in. The state of these high density gluons is also called “Colour Glass Condensate” (CGC) [31]. This new kinematic regime of perturbative QCD at high density at the border to a non-perturbative confinement regime is under intense investigation and is important also for heavy ion collisions where the gluonic state at high density appears initially. Status and applications of the theory of saturation and the CGC are reviewed by *J. Bartels* and *E.G. Ferreira*.

4.2. Evidence for saturation at HERA?

According to the above outline one may reach the saturation region in DIS either by decreasing x at fixed Q^2 , i.e. by increasing the parton density or by decreasing Q^2 at fixed x , i.e. by increasing the parton transverse “size”. In the first case one observes that the structure function F_2 can be well fitted by the NLO QCD in the DGLAP approach for $Q^2 \gtrsim 2 \text{ GeV}^2$ where for $x < 0.01$ one finds an x independent slope $\lambda(Q^2) = -(\partial \ln F_2 / \partial \ln x)_{Q^2}$ which depends linearly on Q^2 . For smaller Q^2 the applicability of the perturbative calculations may be questioned, so there is no direct evidence for saturation in the perturbative regime from this point of view.

On the other hand, a new regime appears in the second case when Q^2 is decreased at fixed x . In this case it is observed that the λ slope saturates for $Q^2 \lesssim 1 \text{ GeV}^2$ (*talk by E. Elsen*). This region of low Q^2 is included in the models of saturation which combine perturbative and non-perturbative aspects. Some essential features of this approach are contained already in the model by Golec-Biernat and Wüsthoff [32]. Here the DIS cross section is obtained in the dipole picture (4) with a simple ansatz for the dipole

cross section $\sigma_{\text{dipole}}(r^2 Q_s^2(x))$ to depend only on the particular combination of r and x and with $Q_s^2(x) \sim x^{-\lambda}$ the saturation scale. The cross section is calculated perturbatively for small distances ($\sigma_{\text{dipole}} \sim r^2$) whereas at large distances a simple Gaussian form has been adopted with saturation built in ($\sigma_{\text{dipole}} \rightarrow \sigma_0$). In this way the full Q^2 range becomes accessible in the model.

An important prediction of the model is the geometrical scaling [33] which states that the cross section $\sigma_{\text{tot}}^{\gamma^* p}(x, Q^2) = f(\tau)$ depends only on the quantity $\tau = Q^2/Q_s^2(x)$. This scaling property is well satisfied.¹ Another successful prediction of the model is the near constancy of the ratio of the diffractive over the full cross section $F_2^{\text{diff}}/F_2^{\text{tot}}$ under variation of the total hadronic mass W .

Recent studies have removed some shortcomings of the model, especially the phenomenological parametrizations for large dipole sizes r . The large Q^2 behaviour can be recovered by a smooth matching to the DGLAP evolution [35]. The solutions of the BK equation determine the behaviour for large r and together with the DGLAP behaviour at small r a good description of HERA data is obtained [36, 37]: the geometrical scaling in the saturation domain, the transition between the hard and soft photon region for the slope λ and the x -dependence of the saturation scale Q_s^2 . These successes in the description of data involving the scale Q_s can be taken as indirect evidence for the onset of saturation.

4.3. Hard diffraction in DIS

Events with a large rapidity gap adjacent to the proton have been observed in NC events with high Q^2 at HERA which are considered as inelastic diffraction of the photon (*K. Borras; C. Kiesling*). Similar events with the charged current have now been reported as well. Assuming Regge factorization for small momentum transfer t between the in and outgoing protons this process can be described by Pomeron exchange where the virtual photon scatters off the Pomeron which is emitted by the incoming proton with momentum fraction $x_{\mathbb{P}} = M_X^2/s$ where M_X denotes the hadronic mass of the $\gamma^* \mathbb{P}$ and \sqrt{s} the cms energy of the $\gamma^* p$ system. In analogy to the standard parton model for ep DIS one can introduce Parton Distribution Functions for the Pomeron [38] to describe $e\mathbb{P}$ DIS. In this “Diffractive DIS” it is possible to derive QCD factorization of the photoabsorption cross

¹ An alternative scaling law has been derived within the framework of a generalized vector-dominance model [34].

section $\gamma^* p \rightarrow pX$ at fixed x_{IP} and momentum transfer t [39]

$$\frac{d^2\sigma^{DDIS}}{dx_{IP}dt} = \sum_q \int_x^{x_{IP}} d\xi f_q^D(x_{IP}, t; \xi, Q^2) \sigma^{\gamma^* q}(x, Q^2, \xi) \quad (5)$$

which further simplifies according to Regge factorization $f_q^D(x_{IP}, t; x, Q^2) = f_{IP/p}(x_{IP}, t) f_{q/IP}(\beta = x/x_{IP}, Q^2)$. These PDF's are then studied as function of $\beta = x_{q/IP}$ or $\beta = x_{g/IP}$ where Bjorken $x = \beta x_{IP}$. Both factorization properties are found to be satisfied by the data but it is necessary to include Reggeon exchange in addition to Pomeron exchange.

The very precise data from the full HERA-I analysis show the rise of the reduced cross section $\hat{\sigma}^{\gamma^* IP}(\beta, Q^2)$ (suitably normalized to correspond to F_2^{ep}) with Q^2 for $\beta \lesssim 0.7$ and the decrease for higher β . The change in slope occurs at much higher value than in case of $\gamma^* p$ scattering. The striking pattern of scaling violation is explained in a NLO DGLAP fit (parameters $\Lambda_{\overline{MS}}$, initial PDF's at $Q_0 = 3$ GeV) by the large gluon fraction in the Pomeron $f_g = 75 \pm 15\%$. QCD factorization is also verified by the observation of diffractive di-jet and charm jet production in agreement with NLO QCD computations using the Pomeron PDF's so obtained.

Theoretical models for the diffractive structure functions (*J. Bartels*) have been developed within the dipole picture with saturation, such as the models by GBW [32] already mentioned and by BEKW [40] which take the higher order QCD processes ($\gamma^* \rightarrow q\bar{q}g$) into account and provide a good description of $F_2^{DDIS}(\beta, Q^2)$.

The structure of simple Feynman diagrams for DDIS has been discussed by *S. Brodsky*. Explicit calculations in case of Feynman gauge for $\gamma^* q \rightarrow s\bar{s}q$ show that the rescattering of the struck s quark involving nearly on-shell intermediate states leads to an imaginary amplitude and an effective Pomeron exchange in the production of the colour singlet $s\bar{s}$ state. This process survives in the Bjorken limit. The same QCD final state interaction also can produce single spin asymmetries in semi-inclusive DIS [41].

4.4. Diffraction in $p\bar{p}$ collisions

Results from the TEVATRON on multi-gap events, hard diffractive processes with jets, $W, Z, J/\psi, B$ have been discussed; exclusive double Pomeron χ_c , $\gamma\gamma$ and di-jet production are of interest as benchmark for exclusive Higgs production at the LHC; the analysis of RUN II data is in progress (reports by *K. Borras, M. Convey, K. Goulianos*).

The factorization of Pomeron processes has been established in DDIS but the arguments cannot be taken over to hadronic processes. In fact, the observed cross sections for diffractive di-jet rates at the Tevatron, are

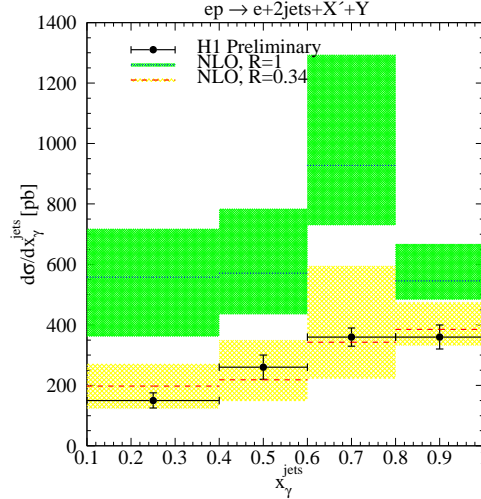


Fig. 3. NLO cross sections for diffractive dijet photoproduction as functions of jet energy fraction x_{γ}^{jets} compared to preliminary H1 data. The predictions including absorption ($R=0.34$ [44]) agree with the data, those without absorption ($R=1$) do not (from Ref. [45]).

suppressed by an order of magnitude as expected using the Pomeron PDF's from HERA assuming factorization [42].

Such a suppression has been expected from reinteraction of spectator partons which yields a reduced gap survival probability, see for example [43]. This idea is supported by the observation of CDF that the occurrence of an additional gap is unsuppressed; by appropriate combination of multi-gap cross sections in soft diffraction the survival probability has been determined as $S = 0.23 \pm 0.07$ at $\sqrt{s} = 1800$ GeV. Taking this effect into account the factorization properties and agreement with extrapolations from HERA can be reestablished. A general systematics of multi-gap events of various kinds with characteristic factorization properties, also in hard processes, has been proposed (*K. Goulianos*) in the framework of a parton model which includes empirical rules like “ $1/M^2$ scaling” and “Pomeron flux renormalization”.

The theoretical approach by KKMR [44] is based on hard QCD scattering processes, but includes initial state interaction by multiple Pomeron exchanges which are derived in a 2-channel eikonal model. This approach explains quantitatively the phenomena of factorization breakdown and the rates of multiple gap events. An interesting prediction concerns the breakdown of factorization in di-jet photoproduction at HERA [44] with an additional suppression $S = 0.34$. This effect has been verified recently in a NLO

QCD calculation [45] in comparison with H1 data [46] (see Fig. 3).

5. Heavy ion collisions and Evidence for Quark Gluon Plasma

Here the transition from a parton to a hadron ensemble is studied in a very high particle multiplicity environment which suggests a thermodynamic treatment. In lattice QCD one expects with increasing temperature T or energy density ϵ a phase transition from confined to deconfined matter, i.e. from a hadron gas to a Quark Gluon Plasma. The ratio ϵ/T^4 , a measure of the number of degrees of freedom, shows a characteristic rise with T near $T_0 \sim 170$ MeV, $\epsilon_0 \sim 0.7$ GeV/fm³, depending also on the number of flavours, over a range of about $\Delta T \sim 80$ MeV and then, above $\epsilon \sim 2$ GeV/fm³, becomes nearly T independent; in this region there is still a large ($\sim 30\%$) deviation from the asymptotic Stefan-Boltzmann limit for the ideal quark-gluon gas [47]. Another prediction concerns the dependence of the critical temperature T_c on the baryochemical potential μ which can be tested through the hadron composition of the final state.

Previous research at the SPS has identified various signatures expected for the transition to a QGP, such as strangeness excess, J/ψ -suppression, universal chemical freeze out; the energy density is found at $\epsilon \sim 2 - 4$ GeV/fm³, just above the critical value. Now with RHIC a new regime with the much higher initial density of ~ 15 GeV/fm³ is reached much above the critical density. This leads to new signatures: a strong asymmetric flow of particles reflecting the initial spacial anisotropy and the strong absorption of high p_T jets in the nucleus (“jet quenching”). It appears particularly impressive with the new RHIC data, that more specific QCD tests are now becoming feasible. A general outline of the RHIC results and their interpretation is given by *R. Seto*.

5.1. Onset of deconfinement in the SPS energy range

Results on AA collisions from an energy scan over the lower SPS energies 20-80 AGeV have been presented by *P. Seyboth*. After the observation of signatures for QGP formation at the top SPS energy the aim was to search for an energy threshold of such signatures.

A remarkable effect is seen in the energy dependence of the freeze out temperature, as determined from the slope of the transverse mass of kaons: at low energies there is a strong rise of temperature followed by saturation over the SPS energy range and continued rise at RHIC energies. This is the typical behaviour expected for a mixed phase of QGP and hadron gas at constant temperature. Such a behaviour at the energy density $\epsilon \gtrsim 2$ GeV/fm³ in the SPS range matches the values expected from lattice calcu-

lations. A threshold effect is also seen for strangeness production, especially the K^+/π^+ ratio which is a well established signature for QGP formation.

Another test of lattice QCD calculations concerns the phase diagram in the variables T vs. baryochemical potential μ_B . The analysis of the particle species abundances in statistical models yields values for T and μ_B at freeze out which converge for low μ_B (high energies) towards the QCD expectation [48].

5.2. Space-time evolution of collision process at RHIC

Initial stage (E.G. Ferreira, K. Tuchin). The initial conditions can be introduced by the gluon density in the nucleus at the saturation scale (see Eq. (3)) as $xG_A(x, Q_s^2) \sim \frac{\pi R_A^2 Q_s^2(x, A)}{\alpha_s(Q_s^2)}$ (“Colour Glass Condensate”) where the A dependence is inferred from $G_A \sim A$, $\pi R_A^2 \sim A^{\frac{2}{3}}$ and $Q_s^2 \sim A^{\frac{1}{3}}$. Assuming proportionality of particle multiplicity and initial gluon rapidity density $dN/dy \sim xG(x, Q_s^2)$ one finds for an AA collision with N_{part} participating nucleons a very slow increase of central hadron multiplicity $(1/N_{part})dN/dy \sim 1/\alpha_s(Q_s^2) \sim \ln N_{part}$ with energy and centrality [49], a very successful prediction; other predictions from parton saturation follow for the transverse momentum distributions (review [50]).

Early interactions: jet production and jet quenching (Miller, Vitev). These new phenomena are related to the hard parton-parton scattering in nuclear collisions and subsequent absorption of one parton in the dense medium. The absorption is mainly due to induced gluon radiative energy loss in multiple scattering inside the nucleus and is proportional to the plasma density [51]. The most striking evidence for jet quenching comes from the study of azimuthal angle correlations of particles associated with a high p_T trigger particle [52]: whereas in both pp and dAu scattering one observes a jet in direction opposite to the trigger jet this away side jet is fully suppressed in central $AuAu$ collisions. This is naturally explained by the hard collision taking place near the edge of the nucleus where one scattered parton leaves the nucleus undisturbed whereas the second parton has to move through the big nucleus. This measurement demonstrates the big difference between cold nuclear matter traversed in dA collisions and the matter created in the central $AuAu$ collision. Theoretical calculations lead to an estimate of energy density of $\epsilon \sim 15$ GeV/fm³ corresponding to about 100 times nuclear density. Additional studies confirm the absorption strength as function of the nuclear thickness in non-central collisions as well as the reappearance of the lost energy of the primary parton in the soft particles in jet direction.

While these observations provide already a strong argument in favour of the presence of a QGP there are further crucial tests. QCD predicts the

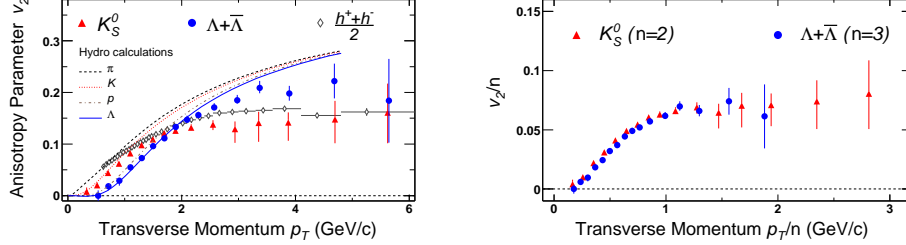


Fig. 4. Transverse momentum dependence of elliptic flow v_2 measured by STAR [55] a) before and b) after rescaling by the number of valence quarks n .

absorption of a gluon to be stronger than that of the quark by the factor C_A/C_F . Furthermore, heavy quarks are less absorbed as the small angle radiation is cut off below $\Theta_c = m_Q/E$ (“dead cone effect”) [53]. This effect is being searched for in nuclear D meson production (Z. Xu).

Hydrodynamic evolution, flow phenomena (Y. Hama, T. Hirano, H. Long, J. Velkowska and S. Voloshin). The hydrodynamics description of the particle production process includes the initial condition (energy density, initial flow), the EoS for the QGP with a phase transition built in (parameter: latent heat) and the freeze out mechanism for hadron production. The observations related to hydrodynamics are:

1. Violation of m_T -scaling in AA collisions, which denotes a universal slope β in $dN/dp_T^2 \sim e^{-\beta m_T}$ for particles of different mass and works well in pp scattering. In hydrodynamic flow the particles acquire similar velocities and therefore protons obtain higher momenta than pions.
2. An important consequence of hydrodynamics is the appearance of an asymmetric, especially elliptic flow: in the non-central collision of two nuclei there is an almond shape overlap region which generates an asymmetric pressure gradient with maximum in impact direction; this results in a corresponding asymmetry in energy and particle flow $\frac{dN}{d\phi} \sim 1 + 2v_2 \cos 2\phi + \dots$. The elliptic flow v_2 increases for particles of higher p_T with a delay for heavier particles.
3. The Equation of State (EoS) can be investigated, especially the properties of the phase transition (latent heat $\sim 800 \text{ MeV/fm}^3$) which provides another QCD test.
4. An apparent problem for the hydrodynamic description is met with the Bose-Einstein correlations between identical particles which depend on the evolution of the space time volume containing the matter. Whereas T. Hirano notes a failure of this description it has been pointed out by T. Csorgö in the discussion that the disagreement can be avoided by a proper choice of the initial transverse flow to explain the final “Hubble flow” (Buda-Lund model [54]).

Coalescence, quark recombination (R. Hwa, J. Velkovska, S. Voloshin).

Another striking new phenomenon observed at RHIC is the grouping of spectra according to the number of constituent quarks. This is observed in the p_T dependence of the elliptic flow parameter v_2 ($p_T < 6$ GeV) where π, K and p, Λ, Ξ fall into separate bands but show a uniform dependence if rescaled according to the number n_V of valence quarks [55, 56]

$$v_2/n_V = f(p_T/n_V). \quad (6)$$

As an example the K, Λ spectra are shown in Fig. 4. Another observation concerns the ratios R_{CP} of particle spectra for central and peripheral collisions where mesons (ϕ, K^0, K^\pm) and baryons (Ω, Ξ, Λ + antiparticles) fall into separate bands in the region $2 \lesssim p_T \lesssim 6$ GeV. This confirms the idea of parton coalescence [57]. There are several other “anomalies” in nuclear production, for example, the large ratio p/π^+ for large $p_T > 2$ GeV which can be explained within a recombination mechanism for thermal and shower partons (R. Hwa).

The behaviour (6) suggests that before hadron formation there is a flow of constituent quarks which then recombine into the observed hadrons. This implies a strong dependence of the q/g composition of the plasma during the evolution as illustrated in Fig. 5 : initially the primary collision produces mainly gluons at high temperature; during the expansion $q\bar{q}$ pairs are produced, but in approaching the critical temperature the gluons are absorbed by the quarks (“constituent quarks”) which then by coalescence form the final state hadrons. The strong ordering according to valence content is against expectations from a hadronic resonance gas which would group particles according to mass. These observations are therefore another strong argument for the presence of a QGP (although at the end without gluons). Looked at in reverse order the evolution depicted in Fig. 5 is quite natural: the hadrons under increased pressure dissolve at first into constituent quarks (as in the additive quark model) but under increased pressure gluons are easily freed from the constituent quarks and yield a genuine QGP.

Strongly interacting QGP. There is another interesting message in the p_T -dependence of the elliptic flow parameter v_2 . Using a calculation for a QGP within transport theory [58] it is found that the gluon-gluon cross sections of few mb expected in pQCD would give negligible flow effects, only cross sections of $\gtrsim 40$ mb would yield the observed asymmetric flow. Therefore, the data suggest a strongly interacting QGP and this can be related to the large deviation from the Stefan-Boltzmann limit of the ideal gas found in the lattice QCD calculations [59].

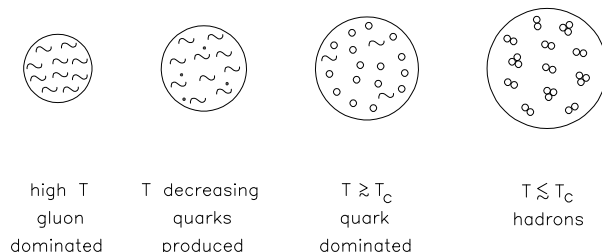


Fig. 5. Evolution of the quark gluon plasma from a gluon dominated phase of high temperature and density towards a quark dominated phase near the critical temperature T_c , finally the transition from constituent quarks to hadrons.

6. Other presentations

Finally, we list a few other topics which have been discussed.

1. *Hadronic Phenomena.* Particle correlations are often not accessible to a QCD description, especially the Bose-Einstein correlations which turn out to be particularly important in the discussion of Heavy Ion Collisions. Also there are discussions of critical phenomena such as percolation and clustering in a string or hadron model framework.

2. *Hadron Spectroscopy.* This is another active field with surprising results on unexpected hadronic particles, including the still controversial “pentaquarks”, especially $\Theta^+(1540)$, not observed at TEVATRON, and the new charmonium state with decay $X(3872) \rightarrow J/\psi \pi^+ \pi^-$ reported here by CDF, which stimulates discussions of nonperturbative aspects of QCD.

3. *Astroparticle Physics.* In this field we witness a flourishing activity where Multiparticle Production plays an important role, although not as the basic goal of the activity but rather as a tool. Primary cosmic particles of superhigh energies (10^8 TeV) are studied. The interpretation of the particle yields, in particular the determination of the primary particle energies requires a detailed understanding of the propagation and showering of the cosmic rays (elementary particles or nuclei) in various media (air, earth, ice), including the saturation phenomena and production and decay of heavy quarks (c, b quarks). Questions of the role of particles in theories beyond the standard model are being discussed, as well as the origin of such high energy cosmic rays.

7. Summary

The number of multiparticle production phenomena which can be explained within QCD is steadily increasing.

1. *Hard processes:* Calculations for larger kinematical ranges, for observables of higher complexity and with increasing accuracy agree with the data, no definitive failures have been reported this time.
2. *Soft particle production:* It follows perturbative QCD expectations surprisingly well which is in support of a parton hadron duality picture of hadronization with soft colour confinement.
3. *Small x and diffraction:* For a high density regime at small Q^2 there is indirect evidence for saturation (“Color Glass Condensate”) inferred from the success of saturation models. Intrinsic Pomeron structure is a useful concept in diffractive scattering, the systematics of factorization and its breaking are becoming better understood.
4. *Heavy Ions and QGP:* There is an indication of a phase transition with a mixed phase over the SPS energy range. The higher initial pressure and longer evolution time available at RHIC have provided clear evidence for jet quenching and strong elliptic flow with an initial energy density about 100 times higher than in nuclear matter and an order of magnitude above critical density. These phenomena are adequately described in terms of a strongly interacting QGP; these observables can be used as new diagnostic tools which allow detailed tests of (perturbative and non-perturbative) QCD predictions: parton type dependence of absorption, Equation of State with latent heat and strong deviation from ideal gas limit, phase diagram T_c vs. μ_B , the initial CGC state. Hadrons are formed by coalescence of constituent quarks which dominate the QGP in its final stage.

Acknowledgement

I would like to thank Bill Gary and his crew for their engagement in organizing this lively meeting which managed to bring together and to mix up the different multiparticle communities to the benefit of all of us. I am also grateful for the helpful discussions with participants of the meeting, especially J. Bartels, V. Khoze, C. Kiesling, N. Schmitz and P. Seyboth.

REFERENCES

- [1] D.J. Gross and F. Wilczek, *Phys. Rev. Lett.* **26**, 1343 (1973);
H.D. Politzer, *Phys. Rev. Lett.* **26**, 1346 (1973).
- [2] N. Kidonakis and R. Vogt, *Eur. Phys. J.* **C33**, S466 (2004).
- [3] V.M. Abazov et al. (D0 Collaboration) *Nature* **429**, 638 (2004).
- [4] S.D. Ellis, Z. Kunszt and D.E. Soper, *Phys. Rev. Lett.* **64**, 2121 (1990).
- [5] W.T. Giele, E.W.N. Glover, D.A. Kosower, *Nucl.Phys.* **B403**, 633 (1993).

- [6] M.L. Mangano, M. Moretti, F. Piccinini, R. Pittau, A.D. Polosa, *JHEP* 0307, 001 (2003).
- [7] G. Marchesini and B.R. Webber, *Nucl.Phys.* **B349**, 635 (1991).
- [8] T. Binoth, J.P. Guillet, E. Pilon and M. Werlen, *Eur.Phys.J.* **C16**, 311 (2000).
- [9] T. Sjöstrand, P. Eden, C. Friberg, L. Lönnblad, G. Miu, S. Mrenna and E. Norrbin, *Comp. Phys. Comm.* **135**, 238 (2001).
- [10] B.A. Kniehl, G. Kramer and B. Pötter, *Nucl.Phys.* **B582**, 514 (2000).
- [11] S. Kretzer, *Phys. Rev.* **D62**, 054001 (2000).
- [12] S. Bethke, arXiv:hep-ex/0407021.
- [13] A.H. Mueller, *Nucl.Phys. B (Proc. Suppl.)* **18C**, 125 (1990); *J.Phys.* **G17**, 1443 (1991).
- [14] S. Catani, M.H. Seymour, *Phys. Lett.* **B378**, 287 (1996), *Nucl. Phys.* **B485**, 291 (1997).
- [15] Yu.L. Dokshitzer and B.R. Webber, *Phys.Lett.* **B352**, 451 (1995); Yu.L. Dokshitzer, G. Marchesini and B.R. Webber, *Nucl.Phys.* **B469**, 93 (1996).
- [16] Yu.L. Dokshitzer, V.A. Khoze and S.I. Troyan, *Phys. Rev.* **D53**, 89 (1996).
- [17] C.F. Berger, T. Kucs and G. Sterman, *Phys. Rev.* **D68**, 014012 (2003).
- [18] M. Dasgupta and G.P. Salam, *Phys. Lett.* **B512**, 323 (2001).
- [19] Yu. Dokshitzer and G. Marchesini, *JHEP* 0303, 040 (2003).
- [20] Banfi, Salam, G. Zanderighi, arXiv:hep-ph/0304148; arXiv:hep-ph/0407286.
- [21] Ya.I. Azimov, Yu.L. Dokshitzer, V.A. Khoze, S.I. Troyan, *Z. Phys.* **C27**, 65 (1985). V.A. Khoze and W. Ochs, *Int. J. Mod. Phys.* **A12**, 2949 (1997).
- [22] G. Abbiendi *et al.* (OPAL Collaboration), *Phys. Rev.* **D69**, 032002 (2004).
- [23] A. Capella *et al.*, *Phys. Rev.* **D61**, 07400 (2000); I.M. Dremin and J.W. Gary, *Phys. Rep.* **349**, 301 (2001).
- [24] S. Lupia and W. Ochs, *Phys. Lett.* **B418**, 214 (1998).
- [25] P. Eden, *Eur. Phys. J.* **C19**, 493 (2001).
- [26] V.A. Khoze, S. Lupia and W. Ochs, *Phys. Lett.* **B394**, 179 (1997); *Eur. Phys. J.* **C5**, 77 (1998).
- [27] J. Abdallah *et al.* (DELPHI Collaboration), arXiv:hep-ex/0410075.
- [28] L.V. Gribov, E.M. Levin and M.G. Ryskin, *Phys. Rep.* **100**, 1 (1983).
- [29] A.H. Mueller, *Nucl. Phys.* **B335**, 115 (1990); N.N. Nikolaev and B.G. Zakharov, *Z. Phys.* **C49**, 607 (1991).
- [30] I. Balitsky, *Nucl. Phys.* **B463**, 99 (1996); Y.V. Kovchegov, *Phys. Rev.* **D60**, 034008 (1999).
- [31] For a review, see E. Iancu and R. Venugopalan, arXiv:hep-ph/0303204.
- [32] K. Golec-Biernat and M. Wüsthoff, *Phys. Rev.* **D59**, 014017 (1999).
- [33] A.M. Staśto, K. Golec-Biernat and J. Kwieciński, *Phys. Rev. Lett.* **86**, 596 (2001).
- [34] D. Schildknecht, B. Surrow and M. Tentyukov, *Phys. Lett.* **B499**, 116 (2001).

- [35] J. Bartels, K. Golec-Biernat and H. Kowalski, *Phys.Rev.* **D66**, 014001 (2002).
- [36] E. Gotsman, E. Levin, M. Lublinsky and U. Maor, *Eur. Phys. J.* **C27**, 411 (2003).
- [37] E. Iancu, K. Itakura and S. Munier, *Phys. Lett.* **B590**, 199 (2004).
- [38] G. Ingelman and P.E. Schlein, *Phys. Lett.* **B152**, 256 (1985).
- [39] J. Collins, *Phys. Rev.* **D57**, 3051 (1998).
- [40] J. Bartels, J.R. Ellis, H. Kowalski, M. Wüsthoff, *Eur. Phys. J.* **C7**, 443 (1999).
- [41] S.J. Brodsky, P. Hoyer, N. Marchal, S. Peine, F. Sannino, *Phys. Rev.* **D65**, 114025 (2002); S.J. Brodsky, D.S. Hwang, I. Schmidt, *Phys. Lett.* **B530**, 99 (2002).
- [42] T. Affolder *et al.* (CDF Collaboration), *Phys. Rev. Lett.* **84**, 5043 (2000).
- [43] J.D. Bjorken, *Phys. Rev.* **D47**, 101 (1993).
- [44] A.B. Kaidalov, V.A. Khoze, A.D. Martin and M.G. Ryskin, *Eur. Phys.J.* **C21**, 521 (2001); *Phys. Lett.* **B567**, 61 (2003).
- [45] M. Klasen and G. Kramer, workshop *DIS 2004*, Strbske Pleso, Slovakia, April 2004, arXiv:hep-ph/0401202.
- [46] H1 Collaboration, paper 987 subm. to *ICHEP 2002*, Amsterdam.
- [47] F. Karsch, E. Laerman and A. Peikert, *Nucl. Phys.* **B605**, 290 (2002).
- [48] Z. Fodor and S. Katz, *JHEP* *0404*, 50 (2004).
- [49] D. Kharzeev and M. Nardi, *Phys. Lett.* **B507**, 121 (2001); D. Kharzeev and E. Levin, *Phys. Lett.* **B523**, 79 (2001).
- [50] E. Levin, “CGC, QCD saturation and RHIC data”; arXiv:hep-ph/0408039.
- [51] M. Gyulassy and M. Plümer, *Nucl. Phys.* **A527**, 641 (1991); M. Plümer M. Gyulassy and X.N. Wang, *Nucl. Phys.* **A590**, 511c (1991).
- [52] J. Adams *et al.* (STAR Collaboration) *Phys. Rev. Lett.* **91**, 072304 (2003).
- [53] Yu.L. Dokshitzer and D.E. Kharzeev, *Phys. Lett.* **B519**, 199 (2001).
- [54] T. Csörgö and B. Lörsstad, *Phys. Rev.* **C54**, 1390 (1996).
- [55] J. Adams *et al.* (STAR Collaboration) *Phys. Rev. Lett.* **92**, 052302 (2004).
- [56] S.S. Adler *et al.* (PHENIX Collaboration), *Phys. Rev. Lett.* **91**, 182301 (2003).
- [57] D. Molnar and S.A. Voloshin, *Phys. Rev. Lett.* **91**, 092301 (2003).
- [58] D. Molnar and M. Gyulassy, *Nucl. Phys.* **A697**, 495 (2002).
- [59] E. Shuryak, *Prog. Part. Nucl. Phys.* **53**, 273 (2004).